

Signal Processing Meets SGD: From Momentum to Filter

¹Zhipeng Yao, ²Guisong Chang, ¹Jiaqi Zhang, ¹Qi Zhang, ^{1,3}Yu Zhang*, ¹Dazhou Li*

¹Shenyang University of Chemical Technology; ²Northeastern University; ³University of Macau

{yiucp; zhangjiaqi678; zhangqi}@outlook.com; {gschang}@mail.neu.edu.cn; {zhangy; lidazhou}@syuct.edu.cn

Abstract

In the field of deep learning, Stochastic Gradient Descent (SGD) and its momentum-based variants are the predominant choices for optimization algorithms. Despite all that, these momentum strategies, which accumulate historical gradients by using a fixed β hyperparameter to smooth the optimization processing, often neglect the potential impact of the variance of historical gradients on the current gradient estimation. In the gradient variance during training, fluctuation indicates the objective function does not meet the Lipschitz continuity condition at all time, which raises the troublesome optimization problem. This paper aims to explore the potential benefits of reducing the variance of historical gradients to make optimizer converge to flat solutions. Moreover, we proposed a new optimization method based on reducing the variance. We employed the Wiener filter theory to enhance the first moment estimation of SGD, notably introducing an adaptive weight to optimizer. Specifically, the adaptive weight dynamically changes along with temporal fluctuation of gradient variance during deep learning model training. Experimental results demonstrated our proposed adaptive weight optimizer, SGDF (Stochastic Gradient Descent With Filter), can achieve satisfactory performance compared with state-of-the-art optimizers.

1. Introduction

In the training process, the optimizer serves as the model's core. The optimizer refines and adjusts model parameters to ensure that the model recognizes the underlying patterns in the data. Beyond updating weights, its role encompasses strategically navigating complex loss landscapes to identify regions offering the best generalization [16]. The optimizer choice influences training efficiency: model convergence speed, generalization to new data, and resilience to data distribution variations [1]. A poor optimizer choice may lead to a model stalling in suboptimal areas or failing to converge,

but a suitable one can hasten learning and ensure robust performance [25]. Hence, continually refining optimization algorithms is crucial for enhancing machine learning model capabilities.

In deep learning, Stochastic Gradient Descent (SGD) [22] and its variants like momentum-based SGD [27], Adam [17], and RMSprop [14] have secured prominent roles. Despite their substantial contributions to deep learning, these methods have inherent drawbacks. These techniques primarily use first-order moment estimation and frequently overlook the historical gradient's pivotal influence on current predictions. Over-reliance on this can result in sluggish convergence and training instability, particularly with high-dimensional, non-convex loss functions common in deep learning [11]. Such characteristics render adaptive learning rate methods prone to entrapment in sharp local minima, which might hinder the model's generalization capability.

Given the aforementioned limitations, we introduce a new optimization technique, SGDF. SGDF leverages signal processing's filter theory to enhance the first moment estimation, striking a balance between historical and current gradient estimates. With its adaptive weighting mechanism, SGDF more effectively fine-tunes gradient estimates throughout the training process, fostering quicker convergence and heightened stability. Initial evaluations on several benchmark datasets indicate that SGDF outperforms many conventional optimization methods, particularly in convergence speed and end model efficacy.

The main contributions of this paper can be summarized as follows:

- We introduce an optimizer that integrates both historical and current gradient data to compute the gradient's variance estimate, addressing the classical SGD method's slow convergence.
- Leveraging a first-moment filter estimation, our approach markedly enhances the adaptive optimization algorithm's generalization, surpassing traditional momentum strategies.
- We construct an innovative theoretical framework that elucidates the tight connection between the stochastic

*Corresponding Author

sampling gradient and the convergence of the algorithm to a flat minimum. This lays a theoretical foundation for capturing the generalization of optimizers. In addition, we give lower bounds on the expectation of Lipschitz’s continuous constant $\mathbb{E}[L_t]$ for different algorithms and show that reducing the variance of the stochastic gradient during the iteration process ensures that the algorithm iterates closer to a low $\mathbb{E}[L_t]$.

2. Related Works And Motivations

The success of deep learning models hinges on the effectiveness of their underlying optimization algorithms in calibrating parameters. Upon closer inspection, a significant challenge emerges. Deep neural networks’ loss landscapes exhibit local minima, saddle points, and plateaus [7]. Navigating these intricate terrains necessitates optimizers that converge swiftly and ensure solutions with robust generalization to new data.

Striving for low training error while maintaining robust generalization epitomizes the bias-variance tradeoff [10]. The trajectory of an optimizer within the loss landscape represents this trade-off. An erratic trajectory might venture into sharp, non-generalizing areas, whereas a conservative one might remain stuck in expansive, suboptimal plateaus [34].

Current literature features numerous optimization techniques, mainly focused on Stochastic Gradient Descent (SGD) variants with adaptive learning rates [8, 33]. Though SGD and its derivatives have advanced in many applications, they come with inherent limitations. They often oscillate or get trapped in sharp minima [29]. Despite achieving low training loss, such minima frequently fail to generalize effectively to new data [12, 30]. This behavior intensifies in the high-dimensional, non-convex terrains characteristic of deep learning settings [4].

Figure 1 provides a visualization to illustrate the behavior of various optimization algorithms. The figure clearly depicts the loss landscapes for Adam, SGD-Momentum, and our proposed optimizer. Notably, the visualization reveals Adam’s propensity to converge to sharper minima.

Recently, the integration of second-order information into optimization problems has gained traction. Techniques like the Extended Kalman Filter [23] incorporate curvature information. The KOALA algorithm [5] stands out, merging loss adaptivity and optimization. It adjusts learning rates considering both gradient magnitudes and the loss landscape’s curvature. These methods offer a nuanced view of the loss landscape, facilitating more informed updates, expedited convergence, and better generalization.

Our research is motivated by these challenges. Despite valuable insights from prior studies, a significant gap persists in comprehensively understanding optimizer behavior, particularly for complex, real-world datasets. We intend

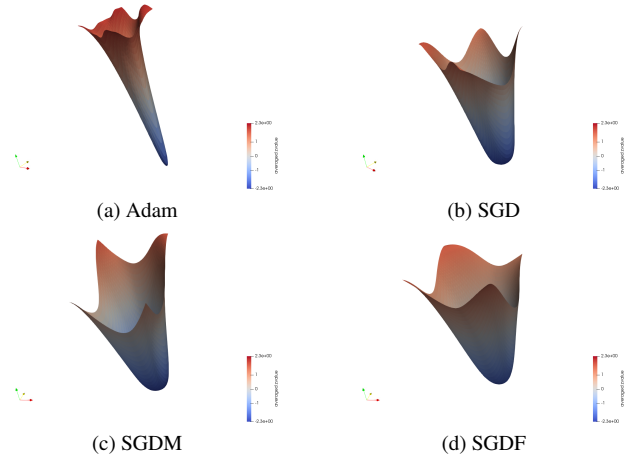


Figure 1. Visualization of loss landscape.

to bridge this gap, offering both theoretical and empirical perspectives on the navigation of optimizers through the loss landscape. Crucially, we investigate the ramifications of such behavior on model generalization.

3. Main Result

3.1. Preliminaries

Definition. Let $f : \mathbb{R}^n \rightarrow \mathbb{R}$ be a differentiable function. The gradient of f is said to be Lipschitz continuous if there exists a non-negative constant L (referred to as the Lipschitz constant of the gradient) such that for all $x, y \in \mathbb{R}^n$, the following inequality holds:

$$\|\nabla f(x) - \nabla f(y)\| \leq L\|x - y\| \quad (1)$$

This constant L describes the rate of change or the bound on the slope of the gradient. A small L implies that the gradient of the function changes slowly, whereas a large L might suggest rapid changes in the gradient in some regions.

For the update rule of SGD:

$$\theta_{t+1} = \theta_t - \alpha \nabla f_s(\theta_t). \quad (2)$$

where α is the learning rate and $\nabla f_s(\theta_t)$ is the gradient calculated based on stochastic sampling from the dataset at each iteration.

Given that we use a stochastic gradient at each iteration, for adjacent iterations, we expect some difference in the gradients. This expected difference is given by:

$$\mathbb{E}[\|\nabla f(\theta_{t+1}) - \nabla f(\theta_t)\|] \leq \alpha \mathbb{E}[L_t] \mathbb{E}[\|\nabla f_s(\theta_t)\|] \quad (3)$$

The inequality suggests that the expected difference in gradients (on the left) is bounded by the expected norm of the gradient of a randomly selected sample (on the right) multiplied by the learning rate and the expected Lipschitz

constant. This bound can provide insights into the stability and convergence properties of the algorithm.

In essence, we're relating the expected difference in gradients to the expected Lipschitz constant of the sample and the expected norm of its gradient. This means that if our function has a high Lipschitz constant over the data distribution, or if our sample gradient has a high expected norm, then our expected gradient difference will also be high.

3.2. L_k lower bound for different algorithms

Theorem 1. Let $f : \mathbb{R}^n \rightarrow \mathbb{R}$ be a differentiable function with its gradient Lipschitz continuous. If, in consecutive SGD iterations, the following inequality holds:

$$\frac{\mathbb{E} [\|\nabla f(\theta_{t+1}) - \nabla f(\theta_t)\|]}{\alpha \mathbb{E} [\|\nabla f_s(\theta_t)\|]} \leq \mathbb{E} [L_t]. \quad (4)$$

Then, applying logarithm to the above inequality and summing from $t = 1$ to T , we obtain:

$$\sum_{t=1}^T \log(\mathbb{E} [L_t]) \leq \sum_{t=1}^T (\log(\mathbb{E} [\|\nabla f(\theta_{T+1}) - \nabla f(\theta_1)\|]) - \log(\alpha \mathbb{E} [\|\nabla f_s(\theta_t)\|])). \quad (5)$$

Theorem 1. elucidates the smoothness properties of the Stochastic Gradient Descent (SGD) algorithm. It posits that, through consecutive SGD iterations, the cumulative difference in gradients remains constant from the initiation to the culmination. This variance is intimately tied to both the magnitude of the gradient at each iterative step and the bounded rate of gradient alteration, characterized by the Lipschitz constant. This offers a quantitative mechanism to gauge the stability of SGD variants, underlining the pivotal role of gradient magnitude and Lipschitz continuity in ensuring the algorithm's smooth behavior.

Similarly, consider the update rule for the momentum method:

$$\begin{aligned} v_{t+1} &= \beta v_t + \alpha \nabla f_s(\theta_t) \\ \theta_{t+1} &= \theta_t - v_{t+1} \end{aligned} \quad (6)$$

For the expectation of the gradient, we have: $\mathbb{E}[\nabla f_s(\theta_t)] = \mathbb{E}[g_t]$. We also derive the expectation of the momentum term:

$$\mathbb{E}[v_{t+1}] = \alpha \sum_{i=0}^t \beta^i \mathbb{E}[g_{t+1-i}] \quad (7)$$

Theorem 2. Given the momentum method, the lower bound of the expected gradient after accumulating over T

time steps is:

$$\begin{aligned} \sum_{t=1}^T \log(\mathbb{E}[L_t]) &\leq \sum_{t=1}^T \left(\log(\mathbb{E} [\|\nabla f(\theta_{T+1}) - \nabla f(\theta_1)\|]) \right. \\ &\quad \left. - \log(\alpha \sum_{i=0}^t \beta^i \mathbb{E} [\|g_{t+1-i}\|]) \right) \end{aligned} \quad (8)$$

Theorem 2. demonstrates that when employing momentum, the bound on the expectation of the loss, L_k , in log space, is determined by the weighted sum of current and previous gradients. Due to this weighted accumulation effect, denoted by β^i , momentum can more effectively leverage historical gradient information.

In comparison to standard SGD, this information enables momentum to more easily escape local minima and saddle points as it updates parameters based not just on the current gradient information but takes into account the direction and magnitude of past gradients. This consideration of past gradients offers a smoothing mechanism, aiding in overcoming challenges arising from noisy gradients or unstable learning dynamics.

Thus, it can be argued that momentum typically results in a lower, more favorable bound on L_k , assisting in accelerating convergence and achieving superior solutions, especially when confronting problems with complex loss landscapes.

Consider the update rules of the Adam method, wherein the update of parameters depends not only on the first moment (i.e., mean) of the gradient but also on its second moment (or an approximation of unbiased variance). Specifically, through the utilization of the mean \hat{m}_t and unbiased variance \hat{v}_t , we arrive at the following approximation for the stochastic gradient:

$$\theta_{t+1} = \theta_t - \alpha \frac{\mathbb{E}[g_t]}{\sqrt{\mathbb{E}^2[g_t] + \text{Var}(g_t)}} \quad (9)$$

Theorem 3. The lower bound for $\mathbb{E}[L_k]$ with the Adam method is then: the stochastic gradient:

$$\begin{aligned} \sum_{t=1}^T \log(\mathbb{E}[L_t]) &\leq \sum_{t=1}^T \left(\log(\mathbb{E} [\|\nabla f(\theta_{T+1}) - \nabla f(\theta_1)\|]) \right. \\ &\quad \left. - \log \left(\alpha \frac{\mathbb{E} [\|g_t\|]}{\sqrt{\mathbb{E}^2 [\|g_t\|] + \text{Var} (\|g_t\|)}} \right) \right) \end{aligned} \quad (10)$$

However, it is critical to note that the adaptive nature of the Adam method may lead it to converge to sharper minima compared to standard SGD, potentially resulting in less robust solutions. Moreover, the variance of the gradient can significantly impact Adam's updates, with unbounded variance potentially leading to instability.

Theorem 4. Let g_t be a stochastic gradient, such that $g_t = \nabla f_s(\theta_t)$. If the variance of the random variable g_t , denoted as $\text{Var}(g_t)$, converges to a certain Cramér-Rao lower bound C , i.e.,

$$\lim_{t \rightarrow \infty} \text{Var}(g_t) = C \quad (11)$$

then, as t increases, we can assert that g_t will unbiasedly approach its expected value $\mathbb{E}[g_t]$, formally stated as:

$$\lim_{t \rightarrow \infty} P(g_t - \mathbb{E}[g_t] = 0) = 1 \quad (12)$$

The variance of the stochastic gradient has a significant effect on the stability and convergence of the SGD algorithm. When the variance of the stochastic gradient decreases, it is more likely to reach its desired value, which helps to maintain the stability of SGD and speed up convergence.

Theorem 1 provides a mechanism for evaluating the stability of SGD, while Theorem 3.2.4 provides insight into understanding how the variance of the gradient affects the stability of the algorithm. This further ensures the smoothness and stability of SGD when the variance of the stochastic gradient converges.

To validate our theory, we examined the Hessian matrix, which describes the second-order curvature of the loss function in parameter space. The Hessian matrix’s eigenvalues offer vital insights into the loss surface’s curvature. Within this framework, we emphasize the Lipschitz constant, as it sets an upper limit on gradient variation. Specifically, a significant Hessian eigenvalue indicates areas of high curvature, potentially corresponding to rapid gradient shifts, directly relating to the Lipschitz constant [2].

We computed the Hessian spectrum of ResNet-18 trained on the CIFAR-100 dataset for 200 epochs. These trainings used SGD, SGDM, Adam and SGDF, which are four optimization methods. We use power iteration [31] to compute the top eigenvalues of Hessian and Hutchinson’s method [32] to compute the Hessian trace. We present histograms depicting the distribution of the top-50 Hessian eigenvalues for each optimization method. We present histograms depicting the distribution of the top-50 Hessian eigenvalues for each optimization method.

These histograms elucidate how different optimization methods influence the Hessian eigenvalues’ distribution, shedding light on their correlation with the Lipschitz continuity.

4. Wiener Filter Estimate Gradient

Based on the above theories, we present SGDF, a novel optimization method. SGDF employs Wiener filtering to minimize the mean squared error [28], which in turn effectively reduces the variance of the estimated gradient distribution. This design ensures that the algorithm converges more steadily to flatter regions.

Algorithm 1: SGDF, Wiener Filter Estimate Method. All operations are element-wise.

Input: $\{\alpha_t\}_{t=1}^T$: step size,
 $\{\beta_1, \beta_2\}$: momentum and adaptive rate coefficients,
 θ_0 : initial parameter,
 $f(\theta)$: stochastic objective function
Output: θ_T : resulting parameters.
Init: $m_0 \leftarrow 0, v_0 \leftarrow 0$
while $t = 1$ to T **do**
 $g_t \leftarrow \nabla_{\theta} f_t(\theta_{t-1})$ (Calculate gradients w.r.t. stochastic objective at timestep t)
 $m_t \leftarrow \beta_1 m_{t-1} + (1 - \beta_1) g_t$ (Calculate momentum)
 $s_t \leftarrow \beta_2 s_{t-1} + (1 - \beta_2) (g_t - m_t)^2$ (Calculate variance)
 $\hat{m}_t \leftarrow \frac{m_t}{1 - \beta_1^t}, \hat{s}_t \leftarrow \frac{s_t}{1 - \beta_2^t}$ (Bias correction)
 $K_t \leftarrow \frac{\hat{s}_t}{\hat{s}_t + (g_t - \hat{m}_t)^2}$ (Calculate Estimate Gain)
 $\hat{g}_t \leftarrow \hat{m}_t + K_t (g_t - \hat{m}_t)$ (Update gradient estimation)
 $\theta_t \leftarrow \theta_{t-1} - \alpha_t \hat{g}_t$ (Update parameters)
return θ_T

4.1. SGDF details

In the SGDF algorithm, the term s_t serves as an important indicator. It is approximated by the exponential moving average of the squared difference between the current gradient g_t and its corresponding momentum m_t . This acts as a proxy for long-term gradient variations, with its weight modulated by the hyperparameter β_2 . In essence, s_t can be interpreted as an estimation of the variance or inherent uncertainty that captures the scale of fluctuations in the gradient.

Regarding the gradient, at any given time step t , g_t denotes the stochastic gradient with respect to our objective function. Concurrently, m_t provides an approximation of the history of the gradient, as it denotes the exponential moving average of the gradient, accumulating past gradient values in a weighted manner. As a result, the term $g_t - m_t$ emerges as a key concept. It can be seen as the “residual” or deviation of the gradient during the optimization process. This deviation essentially shows how much the current gradient diverges from its historical trend. From a Bayesian perspective, this deviation mirrors the uncertainty or intrinsic noise involved in the estimation of the instantaneous gradient, which can be mathematically represented as $p(g_t | \text{data}) \sim \mathcal{N}(g_t; m_t, \sigma_t^2)$ [20].

In the context of Wiener filtering, the Wiener gain K_t is used to balance the contribution between the current

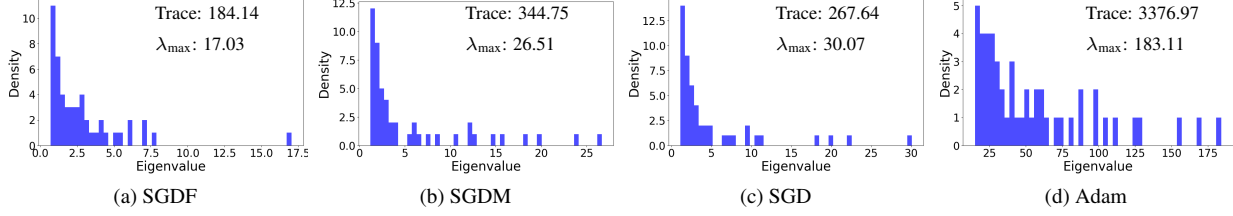


Figure 2. Histogram of Top 50 Hessian Eigenvalues

observed gradient g_t and the past corrected gradient \hat{m}_t , thereby providing a refined gradient estimate. The range of K_t is typically between 0 and 1. It provides a mechanism by which we can balance confidence between the current stochastic gradient and the past corrected gradient. This trade-off is particularly important when dealing with highly noisy gradients or in complex optimisation landscapes. In many deep learning scenarios, gradients are often influenced by various factors, leading to significant noise. By introducing a compensation factor K_t , this noise can be offset to some extent, resulting in a more stable gradient direction, faster convergence and improved model performance. The calculation of K_t is based on the dynamics of s_t and $g_t - m_t$. Its aim is to minimize the expected variance of the corrected gradient estimate \hat{g}_t , which is achieved by optimizing the Wiener filter to obtain optimal linear estimation under noisy conditions.

4.2. Detailed Derivation of the Wiener Gain K_t

The core concept behind the Wiener filter is to provide a linear estimate of a desired signal sequence from another related sequence, so as to minimize the mean square error between the estimated and desired sequences. The Wiener filter operates based on the principles of orthogonality and relies heavily on the statistical properties of the signals involved.

For a clearer understanding, two fundamental concepts related to Wiener filtering are the auto-correlation and cross-correlation of signals:

- **Auto-correlation of a signal:** It measures the similarity between the signal and a delayed version of itself. For the gradient, it's given by $R_g(\tau) = \mathbb{E}[g_t \times g_{t+\tau}]$. where $\mathbb{E}[\cdot]$ denotes the expected value, and τ represents the delay.
- **Cross-correlation between two signals:** It measures the similarity between two signals. For our context, we are interested in the cross-correlation between the original gradient and the noise-augmented gradient $R_{g,g'}(\tau) = \mathbb{E}[g_t \times g'_t]$.

The Wiener-Hopf equation links these concepts and provides the method for solving for the Wiener filter. It's formulated as:

$$R_g(\tau) \times w(\tau) = R_{g,g'}(\tau) \quad (13)$$

Here, $w(\tau)$ represents the weights or coefficients of the Wiener filter.

In the field of optimization, particularly gradient descent, the terrain of the loss landscape can introduce complexities in the trajectory the gradient takes. This can be visualized as noise that perturbs the gradient descent path. Formally, we represent this noise-affected gradient as: $g'_t = g_t + w_k$.

The derivation for K_t starts by understanding its role as a balancing factor between the first and second moments of the gradient. This balancing act ensures that gradient updates are more aligned with the true gradient direction.

Starting with the variance of the corrected gradient, we have:

$$\text{Var}(\hat{g}_t) = (1 - K_t)^2 \text{Var}(\hat{m}_t) + K_t^2 \text{Var}(g_t) \quad (14)$$

The objective is to minimize $\text{Var}(\hat{g}_t)$. Differentiating with respect to K_t and equating to zero, the optimal K_t is found:

$$\frac{\partial \text{Var}(\hat{g}_t)}{\partial K_t} = 2(1 - K_t)\text{Var}(\hat{m}_t) - 2K_t\text{Var}(g_t) = 0 \quad (15)$$

Solving for K_t , we get $K_t = \frac{\text{Var}(\hat{m}_t)}{\text{Var}(\hat{m}_t) + \text{Var}(g_t)}$. Simplifying further, the equation becomes:

$$K_t = \frac{\hat{s}_t}{\hat{s}_t + (g_t - \hat{m}_t)^2}. \quad (16)$$

From the above derivations, it's evident how the principles of Wiener filtering play a significant role in adaptive optimization algorithms, guiding the gradient updates in the presence of noisy landscapes.

4.3. Fusion of Gaussian Distributions

When the Wiener filter is applied, the gradient estimates converge to a Gaussian distribution. The properties of the Wiener filter ensure that the estimated gradient is a linear combination of the current noisy gradient observation g_t and the prior gradient estimate \hat{g}_{t-1} . These two components are assumed to have Gaussian distributions, where $g_i \sim \mathcal{N}(\mu, \sigma^2)$. Hence, their fusion by the Wiener filter naturally results in a Gaussian distribution.

The linearity property of the Wiener filter ensures that the fused estimate \hat{g}_t is also Gaussian. When the Wiener

filter is applied to gradient fusion, the fusion of two Gaussians results in a new Gaussian distribution. Let’s denote the standard deviations of these Gaussians as σ_1 and σ_2 respectively. The variance or standard deviation of the resulting Gaussian distribution is given by the relation

$$\sigma' = \sqrt{\frac{\sigma_1^2 \sigma_2^2}{\sigma_1^2 + \sigma_2^2}} \quad (17)$$

The Gaussian nature of the estimated gradient plays a key role in optimization. This probabilistic representation provides a regularized understanding of the behavior of the gradient. Leveraging this Gaussian assumption helps to model uncertainties in gradient updates, which can lead to more stable and effective optimization trajectories, especially in the complex landscapes associated with deep learning models.

5. Experiments

In this study, We focus on these following tasks: **Image Classification.** We employed the VGG [26], ResNet [13], and DenseNet [15] models for image classification tasks on the Cifar dataset[18]. We evaluated and compared the performance of SGDF with other optimizers such as SGD-Momentum, Adam, RAdam [20], and AdamW [21], all of which were implemented based on the official Pytorch library. Additionally, we further tested the performance of SGDF on the ImageNet dataset [6] using the ResNet model. **Object Detection.** Object detection was performed on the PASCAL VOC dataset using Faster-RCNN integrated with FPN.For hyper-parameter tuning related to image classification and language modeling, refer to [35].Experimental results are given in the following subsection.

Cifar-10/100 Experiments. Initially, we trained on the Cifar-10 and Cifar-100 datasets using the VGG, ResNets, and DenseNet models, and assessed the performance of the SGDF optimizer.We conducted a search for optimal hyper-parameters [35]. For SGD-Momentum, the momentum rate was set to 0.9, and the initial learning rate was 0.1. For Adam, RAdam, and AdamW, we used the default parameters: $lr = 0.001$, $\beta_1 = 0.9$, $\beta_2 = 0.999$, and $\epsilon = 10^{-8}$. For SGDF, the parameters were set as: $lr = 0.3$, $\beta_1 = 0.9$, $\beta_2 = 0.999$, and $\epsilon = 10^{-8}$. In all Cifar-10/100 experiments, the batch size was 128 with basic data augmentation techniques such as random horizontal flip and random cropping (with a 4-pixel padding). We conducted training for 200 epochs, and the learning rate was multiplied by a factor of 0.1 at the 150th epoch. For all optimizers, an typically weight decay of 5×10^{-4} was introduced [21]. The results presented the mean and standard deviation of 3 runs, visualized in curve graphs.

From observing the curve graphs, it is evident that the SGDF optimizer exhibited convergence speeds comparable

to adaptive optimization algorithms. Furthermore, the final test set accuracy achieved by SGDF was either superior to or on par with that of SGD-Momentum.

ImageNet Experiments. In this section, we used the ResNet18 model to train on the ImageNet dataset. Due to extensive computational demands, we did not conduct an exhaustive hyperparameter search for other optimizers and chose to use the best-reported parameters from literature. We trained for 90 epochs using a batch size of 256 and applied basic data augmentation strategies such as random cropping and random horizontal flipping. The learning rate was multiplied by a factor of 0.1 every 30 epochs.For SGDF and SGD-Momentum optimizer, we retained the parameter settings as used in the Cifar experiments.

Object Detection. We do object detection experiments on the PASCAL VOC dataset [9]. The model we used here is pre-trained on COCO dataset [19] and the pre-trained model is from the official website. We train this model on the VOC2007 and VOC2012 trainval dataset (17K) and evaluate on the VOC2007 test dataset (5K).The model we used is Faster-RCNN [24] + FPN. The backbone is ResNet50 [13]. We set the weight decay as 10^{-4} of all methods. We train the model for 4 epochs with batch-size 2 and multiply the learning rates by 0.1 at the last epoch. For all adaptive learning rate methods, the learning rate is set to 10^{-4} ; for SGDM and SGDF, the learning rate is 10^{-2} . Other parameter settings are the same as those in the Cifar Experiments. Results are summarized in Figure and Table. As we except, SGDF outperforms another. These results also illustrates that our method is still efficient in object detection tasks.

6. Conclusion

In this work, we introduced SGDF, a novel optimization method that leverages the information variance of historical gradients combined with current gradients to enhance the gradient estimation process. Through extensive experiments on benchmark datasets like CIFAR-10/100 and ImageNet, using various deep learning architectures such as VGG11, ResNet, and DenseNet, we demonstrated the superior performance of SGDF in comparison to other state-of-the-art optimizers.

Our findings, underscore the importance of considering the variance of historical gradients in the optimization process. By incorporating this perspective, SGDF not only achieves faster convergence but also ensures more stable training, addressing inherent limitations observed in widely-used optimizers such as SGD and Adam. Additionally, the theoretical insights presented highlight the intricate relationship between the variance of gradient distributions and the propensity of algorithms to converge to flat minima. Such insights are pivotal for the deep learning community, emphasizing the significance of flat solutions for improved

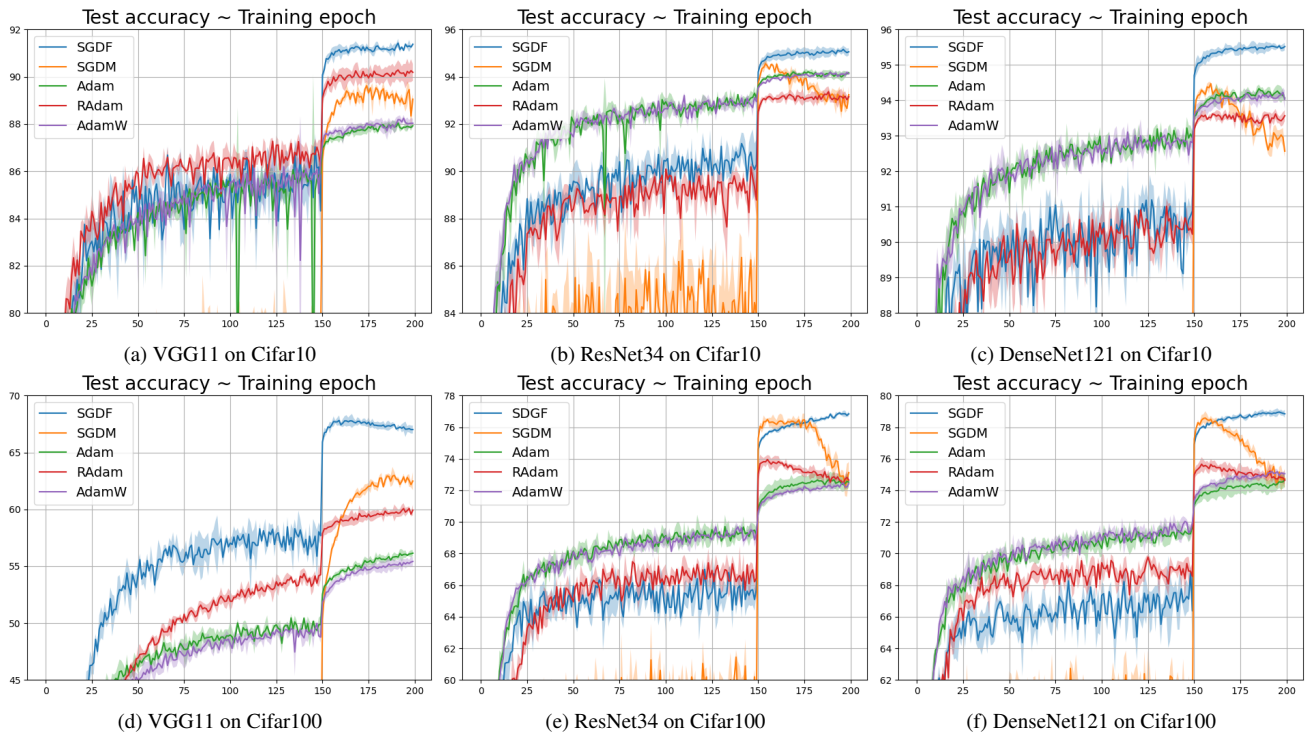


Figure 3. Test accuracy ($[\mu \pm \sigma]$) on Cifar.

Table 1. Top-1 accuracy of ResNet18 on ImageNet. \dagger is reported in [3], \ddagger is reported in [20].

SGDF	SGDM	AdaBound	Yogi	Adam	RAdam	AdamW
68.784	69.73(70.23 \dagger)	68.13 \dagger	68.23 \dagger	63.79 \dagger (66.54 \ddagger)	67.62 \ddagger	67.93 \dagger

generalization.

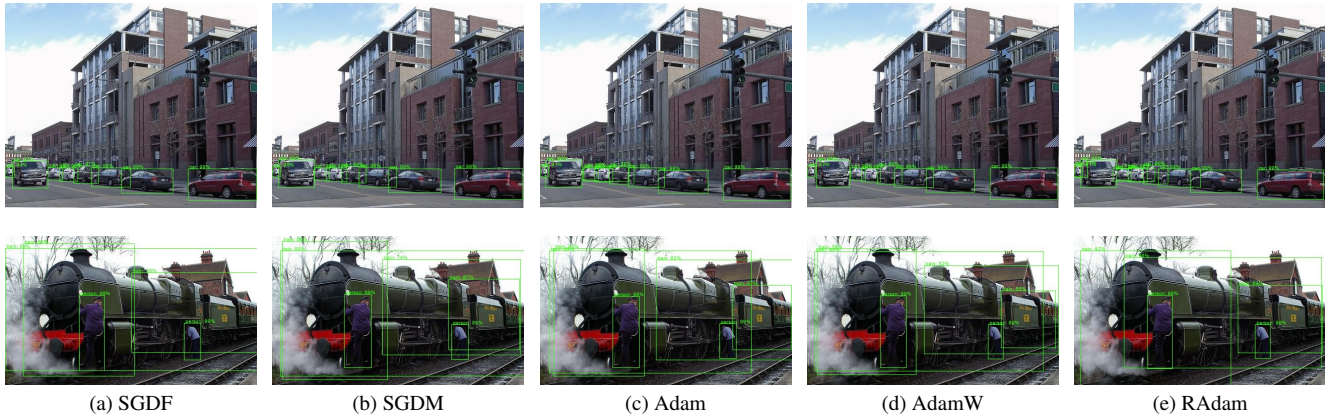
In conclusion, SGDF represents a significant step forward in the realm of optimization algorithms for deep learning. Its ability to strategically navigate the loss landscape, converging to flatter regions, makes it a promising tool for researchers and practitioners aiming for superior model performance and generalization.

References

- [1] Yoshua Bengio and Yann Lecun. Scaling learning algorithms towards ai. 2007. 1
- [2] Debora Caldarola, Barbara Caputo, and Marco Ciccone. Improving generalization in federated learning by seeking flat minima. *ArXiv*, 2022. 4
- [3] Jinghui Chen, Dongruo Zhou, Yiqi Tang, Ziyang Yang, Yuan Cao, and Quanquan Gu. Closing the generalization gap of adaptive gradient methods in training deep neural networks. *arXiv preprint arXiv:1806.06763*, 2018. 7
- [4] Yann Dauphin, Razvan Pascanu, Caglar Gulcehre, Kyunghyun Cho, Surya Ganguli, and Yoshua Bengio. Identifying and attacking the saddle point problem in high-dimensional non-convex optimization. *MIT Press*, 2014. 2
- [5] Aram Davtyan, Sepehr Sameni, Llukman Cerkezi, Givi Meishvili, Adam Bielski, and Paolo Favaro. Koala: A kalman optimization algorithm with loss adaptivity. In *Proceedings of the AAAI Conference on Artificial Intelligence*, pages 6471–6479, 2022. 2
- [6] Jia Deng, Wei Dong, Richard Socher, Li-Jia Li, Kai Li, and Li Fei-Fei. Imagenet: A large-scale hierarchical image database. In *IEEE Conference on Computer Vision and Pattern Recognition*, 2009. 6, 18
- [7] Simon S. Du and Jason D. Lee. On the power of over-parametrization in neural networks with quadratic activation. 2018. 2
- [8] Duchi, John, Hazan, Elad, Singer, and Yoram. Adaptive subgradient methods for online learning and stochastic optimization. *Journal of Machine Learning Research*, 2011. 2
- [9] Mark Everingham, Luc Van Gool, Christopher KI Williams, John Winn, and Andrew Zisserman. The pascal visual object classes (voc) challenge. *International journal of computer vision*, 88(2):303–338, 2010. 6
- [10] Stuart Geman, Elie Bienenstock, and René Doursat. Neural

Method	SGDF	SGDM	Adam	AdamW	RAdam
mAP	83.81	80.43	78.67	78.48	75.21

Table 2. The mAP (higher is better) on PASCAL VOC using Faster-RCNN+FPN.



- networks and the bias/variance dilemma. *Neural Computation*, 4(1):1–58, 2014. 2
- [11] Ian Goodfellow, Yoshua Bengio, and Aaron Courville. *Deep learning*. MIT Press, 2016. 1
- [12] Moritz Hardt, Benjamin Recht, and Yoram Singer. Train faster, generalize better: Stability of stochastic gradient descent. *Mathematics*, 2015. 2
- [13] Kaiming He, Xiangyu Zhang, Shaoqing Ren, and Jian Sun. Deep residual learning for image recognition. In *Proceedings of the IEEE conference on computer vision and pattern recognition*, pages 770–778, 2016. 6, 18
- [14] Geoffrey Hinton. Neural networks for machine learning. Coursera video lectures, 2012. Lecture 6.5 - rmsprop: Divide the gradient by a running average of its recent magnitude. 1
- [15] Gao Huang, Zhuang Liu, Laurens Van Der Maaten, and Kilian Q Weinberger. Densely connected convolutional networks. In *Proceedings of the IEEE conference on computer vision and pattern recognition*, pages 4700–4708, 2017. 6, 18
- [16] Nitish Shirish Keskar, Dheevatsa Mudigere, Jorge Nocedal, Mikhail Smelyanskiy, and Ping Tak Peter Tang. On large-batch training for deep learning: Generalization gap and sharp minima. 2016. 1
- [17] Diederik P Kingma and Jimmy Ba. Adam: A method for stochastic optimization. *arXiv preprint arXiv:1412.6980*, 2014. 1, 18
- [18] Alex Krizhevsky, Geoffrey Hinton, et al. Learning multiple layers of features from tiny images. 2009. 6, 18
- [19] Tsung-Yi Lin, Michael Maire, Serge Belongie, James Hays, Pietro Perona, Deva Ramanan, Piotr Dollár, and C. Lawrence Zitnick. Microsoft coco: Common objects in context. *European Conference on Computer Vision (ECCV)*, 2014. 6
- [20] Liyuan Liu, Haoming Jiang, Pengcheng He, Weizhu Chen, Xiaodong Liu, Jianfeng Gao, and Jiawei Han. On the variance of the adaptive learning rate and beyond. *arXiv preprint arXiv:1908.03265*, 2019. 4, 6, 7, 18, 19
- [21] Ilya Loshchilov and Frank Hutter. Decoupled weight decay regularization. *arXiv preprint arXiv:1711.05101*, 2017. 6, 18
- [22] Robbins Sutton Monro. a stochastic approximation method. *Annals of Mathematical Statistics*, 22(3):400–407, 1951. 1, 18
- [23] Yann Ollivier. The extended kalman filter is a natural gradient descent in trajectory space. *arXiv: Optimization and Control*, 2019. 2
- [24] Shaoqing Ren, Kaiming He, Ross Girshick, and Jian Sun. Faster r-cnn: Towards real-time object detection with region proposal networks. *Neural Information Processing Systems (NIPS)*, 2015. 6
- [25] Sebastian Ruder. An overview of gradient descent optimization algorithms. 2016. 1
- [26] Karen Simonyan and Andrew Zisserman. Very deep convolutional networks for large-scale image recognition. *Computer Science*, 2014. 6, 18
- [27] Ilya Sutskever, James Martens, George Dahl, and Geoffrey Hinton. On the importance of initialization and momentum in deep learning. In *International conference on machine learning*, pages 1139–1147. PMLR, 2013. 1
- [28] Norbert Wiener. The extrapolation, interpolation and smoothing of stationary time series, with engineering applications. *Journal of the Royal Statistical Society Series A (General)*, 1950. 4
- [29] Ashia C. Wilson, Rebecca Roelofs, Mitchell Stern, Nathan Srebro, and Benjamin Recht. The marginal value of adaptive gradient methods in machine learning. 2017. 2
- [30] Zeke Xie, Qian Yuan Tang, Yunfeng Cai, Mingming Sun, and Ping Li. On the power-law spectrum in deep learning: A bridge to protein science. 2022. 2
- [31] Zhewei Yao, Amir Gholami, Qi Lei, Kurt Keutzer, and Michael W. Mahoney. Hessian-based analysis of large batch training and robustness to adversaries. 2018. 4
- [32] Zhewei Yao, Amir Gholami, Kurt Keutzer, and Michael W. Mahoney. Pyhessian: Neural networks through the lens of

the hessian. In *International Conference on Big Data*, 2020. 4

- [33] Matthew D. Zeiler. Adadelat: An adaptive learning rate method. *arXiv e-prints*, 2012. 2
- [34] Chiyuan Zhang, Samy Bengio, Moritz Hardt, Benjamin Recht, and Oriol Vinyals. Understanding deep learning requires rethinking generalization. 2016. 2
- [35] Juntang Zhuang, Tommy Tang, Yifan Ding, Sekhar C Tatikonda, Nicha Dvornek, Xenophon Papademetris, and James Duncan. Adabelief optimizer: Adapting stepsizes by the belief in observed gradients. *Advances in neural information processing systems*, 33:18795–18806, 2020. 6, 18

A. Appendix 1

A.1. Theorem proof.

Assumption: For different algorithms, the initial gradient $\nabla f(\theta_1)$ is a constant value, and $\nabla f(\theta_{T+1})$ converges to a specific value.

Given this assumption, we can further clarify the previous inequality:

Since the initial gradient $\nabla f(\theta_1)$ is a constant value for all algorithms, and $\nabla f(\theta_{T+1})$ converges to a specific value, we can represent:

$$\mathbb{E} [\|\nabla f(\theta_1)\|] = C_1, \text{ and } \mathbb{E} [\|\nabla f(\theta_{T+1})\|] = C_2 \quad (18)$$

where C_1 and C_2 are constants.

Definition 1:(Lipschitz continuous),if f is Lipschitz continuous.

$$\|\nabla f(\mathbf{x}) - \nabla f(\mathbf{y})\| \leq L\|\mathbf{x} - \mathbf{y}\|, \forall \mathbf{x}, \mathbf{y} \in \mathbb{R}^d \quad (19)$$

Theorem 1. With this assumption, given a loss function f and $\nabla f_s(\theta_t)$ is the gradient calculated based on stochastic sampling from the dataset at each iteration, for each step of the update rule of stochastic gradient descent, there is the following inequality relation:

$$\sum_{t=1}^T \log(\mathbb{E}[L_t]) \leq \sum_{t=1}^T (\log(\mathbb{E}[\|\nabla f(\theta_{T+1}) - \nabla f(\theta_1)\|]) - \log(\alpha \mathbb{E}[\|\nabla f_s(\theta_t)\|])) \quad (20)$$

Proof. For the update rule of SGD:

$$\theta_{t+1} = \theta_t - \alpha \nabla f_s(\theta_t). \quad (21)$$

Consider adjacent step iterations, We can derive:

$$\mathbb{E} [\|\nabla f(\theta_{t+1}) - \nabla f(\theta_t)\|] \leq \alpha \mathbb{E}[L_t] \mathbb{E} [\|\nabla f_s(\theta_t)\|] \quad (22)$$

We first apply the logarithm to the whole term and then add up the result.

For the original inequality

$$\frac{\mathbb{E} [\|\nabla f(\theta_{t+1}) - \nabla f(\theta_t)\|]}{\alpha \mathbb{E} [\|\nabla f_s(\theta_t)\|]} \leq \mathbb{E}[L_t] \quad (23)$$

Start by taking logarithms on both sides of the inequality:

$$\log\left(\frac{\mathbb{E} [\|\nabla f(\theta_{t+1}) - \nabla f(\theta_t)\|]}{\alpha \mathbb{E} [\|\nabla f_s(\theta_t)\|]}\right) \leq \log(\mathbb{E}[L_t]) \quad (24)$$

By the logarithmic property, the above inequality can be further transformed into:

$$\log(\mathbb{E} [\|\nabla f(\theta_{t+1}) - \nabla f(\theta_t)\|]) - \log(\alpha \mathbb{E} [\|\nabla f_s(\theta_t)\|]) \leq \log(\mathbb{E}[L_t]) \quad (25)$$

Now add up from $t=1$ to T :

$$\sum_{t=1}^T (\log(\mathbb{E} [\|\nabla f(\theta_{t+1}) - \nabla f(\theta_t)\|]) - \log(\alpha \mathbb{E} [\|\nabla f_s(\theta_t)\|])) \leq \sum_{t=1}^T \log(\mathbb{E}[L_t]) \quad (26)$$

Next, you can replace the difference of successive gradients with the difference in gradients between θ_{T+1} and θ_1 using a triangular inequality. This will find an upper bound for the numerator. Consider the cumulative inequality we have just obtained:

$$\sum_{t=1}^T (\log(\mathbb{E} [\|\nabla f(\theta_{t+1}) - \nabla f(\theta_t)\|]) - \log(\alpha \mathbb{E} [\|\nabla f_s(\theta_t)\|])) \leq \sum_{t=1}^T \log(\mathbb{E}[L_t]) \quad (27)$$

We wish to replace the numerator of the left-hand side with $\mathbb{E}[\|\nabla f(\theta_{T+1}) - \nabla f(\theta_1)\|]$. We already know that the difference in each successive gradient will be less than this according to the trigonometric inequality. Therefore, we have:

$$\mathbb{E}[\|\nabla f(\theta_{t+1}) - \nabla f(\theta_t)\|] \leq \mathbb{E}[\|\nabla f(\theta_{T+1}) - \nabla f(\theta_1)\|] \quad (28)$$

Considering that logarithmic functions are increasing functions, we can apply to the above inequality to get:

$$\log(\mathbb{E}[\|\nabla f(\theta_{t+1}) - \nabla f(\theta_t)\|]) \leq \log(\mathbb{E}[\|\nabla f(\theta_{T+1}) - \nabla f(\theta_1)\|]) \quad (29)$$

Replacing this back into our cumulative inequality, we get:

$$\sum_{t=1}^T \log(\mathbb{E}[L_t]) \leq \sum_{t=1}^T (\log(\mathbb{E}[\|\nabla f(\theta_{T+1}) - \nabla f(\theta_1)\|]) - \log(\alpha \mathbb{E}[\|\nabla f_s(\theta_t)\|])) \quad (30)$$

Theorem 2. With this assumption, given a loss function f and its stochastic gradient ∇f_s , for each step of the update rule of the momentum method, there is the following inequality relation:

$$\sum_{t=1}^T \log(\mathbb{E}[L_t]) \leq \sum_{t=1}^T \left(\log(\mathbb{E}[\|\nabla f(\theta_{T+1}) - \nabla f(\theta_1)\|]) - \log\left(\alpha \sum_{i=0}^t \beta^i \mathbb{E}[\|g_{t+1-i}\|]\right) \right) \quad (31)$$

Proof. The basic update rule for the momentum method is:

$$\begin{aligned} v_{t+1} &= \beta v_t + \alpha \nabla f_s(\theta_t) \\ \theta_{t+1} &= \theta_t - v_{t+1} \end{aligned} \quad (32)$$

For the expectation of the gradient, we have:

$$\mathbb{E}[\nabla f_s(\theta_t)] = \mathbb{E}[g_t] \quad (33)$$

Consider the desired update rule:

$$\mathbb{E}[v_{t+1}] = \beta \mathbb{E}[v_t] + \alpha \mathbb{E}[g_t] \quad (34)$$

Since we already know that $\mathbb{E}[g_t]$ is the expectation of the gradient, we only need to consider the expectation of v_t . When we initialise, $v_0 = 0$, then:

$$\begin{aligned} \mathbb{E}[v_1] &= \alpha \mathbb{E}[g_1] \\ \mathbb{E}[v_2] &= \beta \alpha \mathbb{E}[g_1] + \alpha \mathbb{E}[g_2] \\ \mathbb{E}[v_3] &= \beta^2 \alpha \mathbb{E}[g_1] + \beta \alpha \mathbb{E}[g_2] + \alpha \mathbb{E}[g_3] \end{aligned} \quad (35)$$

As can be seen, at each step the previous gradient is multiplied by an additional β factor. At the t time step, the updated expectation can be written as:

$$\mathbb{E}[v_t] = \alpha \sum_{i=0}^{t-1} \beta^i \mathbb{E}[g_{t-i}] \quad (36)$$

Given an update rule:

$$\mathbb{E}[v_{t+1}] = \beta \mathbb{E}[v_t] + \alpha \mathbb{E}[g_t] \quad (37)$$

At the t time step, the desired update can be expressed as:

$$\mathbb{E}[v_t] = \alpha \sum_{i=0}^{t-1} \beta^i \mathbb{E}[g_{t-i}] \quad (38)$$

Replacing the above equation, we get:

$$\mathbb{E}[v_{t+1}] = \beta \left(\alpha \sum_{i=0}^{t-1} \beta^i \mathbb{E}[g_{t-i}] \right) + \alpha \mathbb{E}[g_t] \quad (39)$$

Expanding and adjusting the index of the summation, we get:

$$\begin{aligned} \mathbb{E}[v_{t+1}] &= \alpha \beta \sum_{i=0}^{t-1} \beta^i \mathbb{E}[g_{t-i}] + \alpha \mathbb{E}[g_t] \\ &= \alpha \sum_{i=1}^t \beta^i \mathbb{E}[g_{t+1-i}] + \alpha \mathbb{E}[g_t] \end{aligned} \quad (40)$$

Now merge similar terms in the above expression:

$$\mathbb{E}[v_{t+1}] = \alpha \sum_{i=0}^t \beta^i \mathbb{E}[g_{t+1-i}] \quad (41)$$

We arrive at a lower bound for the $\sum_{t=1}^T \log(\mathbb{E}[L_t])$ of the momentum method:

$$\sum_{t=1}^T \log(\mathbb{E}[L_t]) \leq \sum_{t=1}^T \left(\log(\mathbb{E}[\|\nabla f(\theta_{T+1}) - \nabla f(\theta_1)\|]) - \log\left(\alpha \sum_{i=0}^t \beta^i \mathbb{E}[\|g_{t+1-i}\|]\right) \right) \quad (42)$$

Theorem 3. With this assumption, given a loss function f and its stochastic gradient ∇f_{s_k} , for each step of the update rule of the Adam method, there is the following inequality relation:

$$\sum_{t=1}^T \log(\mathbb{E}[L_t]) \leq \sum_{t=1}^T \left(\log(\mathbb{E}[\|\nabla f(\theta_{T+1}) - \nabla f(\theta_1)\|]) - \log\left(\alpha \frac{\mathbb{E}[\|g_t\|]}{\sqrt{\mathbb{E}^2[\|g_t\|] + \text{Var}(\|g_t\|)}}\right) \right) \quad (43)$$

Proof. Consider Adam's update method:

$$\begin{aligned} m_t &= \beta_1 m_{t-1} + (1 - \beta_1) g_t \\ v_t &= \beta_2 v_{t-1} + (1 - \beta_2) g_t^2 \\ \hat{m}_t &= \frac{m_t}{1 - \beta_1^t} \\ \hat{v}_t &= \frac{v_t}{1 - \beta_2^t} \\ \theta_{t+1} &= \theta_t - \alpha \frac{\hat{m}_t}{\sqrt{\hat{v}_t} + \epsilon} \end{aligned} \quad (44)$$

The stochastic gradient approximation used by the Adam method for updating:

$$\theta_{t+1} = \theta_t - \alpha \frac{\mathbb{E}[g_t]}{\sqrt{\mathbb{E}[g_t^2]}} \quad (45)$$

By definition of variance:

$$\text{Var}(g_t) = \mathbb{E}[g_t^2] - \mathbb{E}^2[g_t] \quad (46)$$

Since we have:

$$\theta_{t+1} = \theta_t - \alpha \frac{\mathbb{E}[g_t]}{\sqrt{\mathbb{E}^2[g_t] + \text{Var}(g_t)}} \quad (47)$$

We arrive at a lower bound for Adam's method $\sum_{t=1}^T \log(\mathbb{E}[L_t])$:

$$\sum_{t=1}^T \log(\mathbb{E}[L_t]) \leq \sum_{t=1}^T \left(\log(\mathbb{E}[\|\nabla f(\theta_{T+1}) - \nabla f(\theta_1)\|]) - \log\left(\alpha \frac{\mathbb{E}[\|g_t\|]}{\sqrt{\mathbb{E}^2[\|g_t\|] + \text{Var}(\|g_t\|)}}\right) \right) \quad (48)$$

Assumption

$$\lim_{t \rightarrow \infty} \text{Var}(g_t) = C \quad (49)$$

where C is the Cramér-Rao lower bound.

Theorem 4.

$$\lim_{t \rightarrow \infty} P(g_t - \mathbb{E}[g_t] = 0) = 1 \quad (50)$$

Proof. $g_t = \nabla f_s(\theta_t)$: Represents the stochastic gradient. $\xi_t = g_t - \mathbb{E}[g_t]$: Represents the bias, satisfying $\mathbb{E}[\xi_t] = 0$. From the assumption, we know:

$$\lim_{t \rightarrow \infty} \text{Var}(\xi_t) = \lim_{t \rightarrow \infty} \text{Var}(g_t) = C \quad (51)$$

This is due to $\xi_t = g_t - \mathbb{E}[g_t]$.

From the definition of variance, we have:

$$\text{Var}(\xi_t) = \mathbb{E}[\xi_t^2] - \mathbb{E}[\xi_t]^2 \quad (52)$$

But since $\mathbb{E}[\xi_t] = 0$, we can infer:

$$\text{Var}(\xi_t) = \mathbb{E}[\xi_t^2] \quad (53)$$

Therefore, we can deduce:

$$\lim_{t \rightarrow \infty} \mathbb{E}[\xi_t^2] = C \quad (54)$$

Using the Markov inequality, we can state:

$$P(|\xi_t| \geq \epsilon) \leq \frac{\mathbb{E}[\xi_t^2]}{\epsilon^2} \quad (55)$$

As $t \rightarrow \infty$, given that $\mathbb{E}[\xi_t^2]$ approaches C , for any small $\epsilon > 0$, $P(|\xi_t| \geq \epsilon)$ approaches 0. This implies ξ_t tends to 0. As $\xi_t = g_t - \mathbb{E}[g_t]$, it's implied that g_t approaches $\mathbb{E}[g_t]$.

A.2. Proof of Convergence.

Assumption

- Variables are bounded: $\exists B$ such that $\forall t, \|\theta_t\|_2 \leq B$
- Gradients are bounded: $\exists G$ such that $\forall t, \|g_t\|_2 \leq G$

Statistics Let L_t be the loss at time t and L_t^* be the loss of the best possible strategy at the same time. The cumulative regret $R(T)$ at time T is defined as:

$$R(T) = \sum_{t=1}^T L_t - L_t^* \quad (56)$$

Definition 2 If a function $f: R^d \rightarrow R$ is convex if for all $x, y \in R^d$ for all $\lambda \in [0, 1]$,

$$\lambda f(x) + (1 - \lambda)f(y) \geq f(\lambda x + (1 - \lambda)y) \quad (57)$$

Also, notice that a convex function can be lower bounded by a hyperplane at its tangent.

Lemma 2 If a function $f : R^d \rightarrow R$ is convex, then for all $x, y \in R^d$,

$$f(y) \geq f(x) + \nabla f(x)^T (y - x) \quad (58)$$

The above lemma can be used to upper bound the regret and our proof for the main theorem is constructed by substituting the hyperplane with the Algorithm 1 update rules.

The following two lemmas are used to support our main theorem. We also use some definitions simplify our notation, where $g_t \triangleq \nabla f_t(\theta_t)$ and $g_{t,i}$ as the d^{th} element. We define $g_{1:t,d} \in \mathbb{R}^t$ as a vector that contains the d^{th} dimension of the gradients over all iterations till t , $g_{1:t,d} = [g_{1,d}, g_{2,d}, \dots, g_{t,d}]$

Lemma 3. Let $g_t = \nabla f_t(\theta_t)$ and $g_{1:t}$ be defined as above and bounded,

$$\|g_t\|_2 \leq G, \|g_t\|_\infty \leq G_\infty. \quad (59)$$

Then,

$$\sum_{t=1}^T g_{t,d} \leq 2G_\infty \|g_{1:T,d}\|_2. \quad (60)$$

Proof. We will prove the inequality using induction over T . For the base case $T = 1$:

$$g_{1,d} \leq 2G_\infty \|g_{1,d}\|_2. \quad (61)$$

Assuming the inductive hypothesis holds for $T - 1$, for the inductive step:

$$\begin{aligned} \sum_{t=1}^T g_{t,d} &= \sum_{t=1}^{T-1} g_{t,d} + g_{T,d} \\ &\leq 2G_\infty \|g_{1:T-1,d}\|_2 + g_{T,d} \\ &= 2G_\infty \sqrt{\|g_{1:T,d}\|_2^2 - g_{T,d}^2} + g_{T,d}. \end{aligned} \quad (62)$$

Given,

$$\|g_{1:T,d}\|_2^2 - g_{T,d}^2 + \frac{g_{T,d}^4}{4 \|g_{1:T,d}\|_2^2} \geq \|g_{1:T,d}\|_2^2 - g_{T,d}^2, \quad (63)$$

taking the square root of both sides, we get:

$$\begin{aligned} \sqrt{\|g_{1:T,d}\|_2^2 - g_{T,d}^2} &\leq \|g_{1:T,d}\|_2 - \frac{g_{T,d}^2}{2 \|g_{1:T,d}\|_2} \\ &\leq \|g_{1:T,d}\|_2 - \frac{g_{T,d}^2}{2\sqrt{G_\infty^2}}. \end{aligned} \quad (64)$$

Substituting into the previous inequality:

$$G_\infty \sqrt{\|g_{1:T,d}\|_2^2 - g_{T,d}^2} + \sqrt{g_{T,d}^2} \leq 2G_\infty \|g_{1:T,d}\|_2 \quad (65)$$

Lemma 4. Let bounded g_t , $\|g_t\|_2 \leq G$, $\|g_t\|_\infty \leq G_\infty$, the following inequality holds

$$\sum_{t=1}^T \hat{m}_{t,d}^2 \leq \frac{4G_\infty^2}{(1-\beta_1)^2} \|g_{1:T,d}\|_2^2 \quad (66)$$

Proof. Under the inequality: $\frac{1}{(1-\beta_1^t)^2} \leq \frac{1}{(1-\beta_1)^2}$. We can expand the last term in the summation using the update rules in Algorithm 1,

$$\begin{aligned}
\sum_{t=1}^T \widehat{m}_{t,i}^2 &= \sum_{t=1}^{T-1} \widehat{m}_{t,d}^2 + \frac{\left(\sum_{k=1}^T (1-\beta_1) \beta_1^{T-k} g_{k,i}\right)^2}{(1-\beta_1^T)^2} \\
&\leq \sum_{t=1}^{T-1} \widehat{m}_{t,d}^2 + \frac{\sum_{k=1}^T T \left((1-\beta_1) \beta_1^{T-k} g_{k,d}\right)^2}{(1-\beta_1^T)^2} \\
&\leq \sum_{t=1}^{T-1} \widehat{m}_{t,d}^2 + \frac{(1-\beta_1)^2}{(1-\beta_1^T)^2} \sum_{k=1}^T T (\beta_1^2)^{T-k} \|g_{k,d}\|_2^2 \\
&\leq \sum_{t=1}^{T-1} \widehat{m}_{t,d}^2 + T \sum_{k=1}^T (\beta_1^2)^{T-k} \|g_{k,d}\|_2^2
\end{aligned} \tag{67}$$

Similarly, we can upper bound the rest of the terms in the summation.

$$\begin{aligned}
\sum_{t=1}^T \widehat{m}_{t,d}^2 &\leq \sum_{t=1}^T \|g_{t,d}\|_2^2 \sum_{j=0}^{T-t} t \beta_1^j \\
&\leq \sum_{t=1}^T \|g_{t,d}\|_2^2 \sum_{j=0}^T t \beta_1^j
\end{aligned} \tag{68}$$

For $\beta_1 < 1$, using the upper bound on the arithmetic-geometric series, $\sum_t t \beta_1^t < \frac{1}{(1-\beta_1)^2}$:

$$\sum_{t=1}^T \|g_{t,d}\|_2^2 \sum_{j=0}^T t \beta_1^j \leq \frac{1}{(1-\beta_1)^2} \sum_{t=1}^T \|g_{t,d}\|_2^2 \tag{69}$$

Apply Lemma 3,

$$\sum_{t=1}^T \widehat{m}_{t,d}^2 \leq \frac{4G_\infty^2}{(1-\beta_1)^2} \|g_{1:T,d}\|_2^2 \tag{70}$$

Proof of Convergence. We aim to prove the convergence of the algorithm by showing that $R(T)$ is bounded, or equivalently, that $\frac{R(T)}{T}$ converges to zero as T goes to infinity.

To express the cumulative regret in terms of each dimension, let $L_{t,d}$ and $L_{t,d}^*$ represent the loss and the best strategy's loss for the d th dimension, respectively. Define $R_{T,d}$ as:

$$R_{T,d} = \sum_{t=1}^T L_{t,d} - L_{t,d}^* \tag{71}$$

Then, the overall regret $R(T)$ can be expressed in terms of all dimensions D as:

$$R(T) = \sum_{d=1}^D R_{T,d} \tag{72}$$

Establishing the Connection: From the Iteration of θ_t to $\langle g_t, \theta_t - \theta^* \rangle$

Using Lemma 2, we have,

$$f_t(\theta_t) - f_t(\theta^*) \leq g_t^T(\theta_t - \theta^*) = \sum_{i=1}^d g_{t,d}(\theta_{t,d} - \theta_{i,d}^*) \tag{73}$$

From the update rules presented in algorithm 1,

$$\begin{aligned}\theta_{t+1} &= \theta_t - \alpha_t \widehat{g}_t \\ &= \theta_t - \alpha_t (\widehat{m}_t + K_{t,d}(g_t - \widehat{m}_t))\end{aligned}\tag{74}$$

We focus on the i^{th} dimension of the parameter vector $\theta_t \in R^d$. Subtract the scalar $\theta_{*,d}^*$ and square both sides of the above update rule, we have,

$$(\theta_{t+1,d} - \theta_{*,d}^*)^2 = (\theta_{t,d} - \theta_{*,d}^*)^2 - 2\alpha_t(\widehat{m}_{t,d} + K_{t,d}(g_{t,d} - \widehat{m}_{t,d}))(\theta_{t,d} - \theta_{*,d}^*) + \alpha_t^2 \widehat{g}_t^2\tag{75}$$

Separating items $g_{t,d}(\theta_{t,d} - \theta_{*,d}^*)$:

$$g_{t,d}(\theta_{t,d} - \theta_{*,d}^*) = \frac{(\theta_{t,d} - \theta_{*,d}^*)^2 - (\theta_{t+1,d} - \theta_{*,d}^*)^2}{2\alpha_t K_{t,d}} - \frac{1 - K_{t,d}}{K_{t,d}} \widehat{m}_{t,d} (\theta_{t,d} - \theta_{*,d}^*) + \frac{\alpha_t}{2K_{t,d}} (\widehat{g}_{t,d})^2\tag{76}$$

For the first term, we have:

$$\begin{aligned}& \sum_{t=1}^T \frac{(\theta_{t,d} - \theta_{*,d}^*)^2 - (\theta_{t+1,d} - \theta_{*,d}^*)^2}{2\alpha_t K_{t,d}} \\ & \leq \sum_{t=1}^T \frac{(\theta_{t,d} - \theta_{*,d}^*)^2 - (\theta_{t+1,d} - \theta_{*,d}^*)^2}{2\alpha_t K_{t,d}} \\ & = \frac{(\theta_{1,d} - \theta_{*,d}^*)^2}{2\alpha_1 K_{1,d}} - \frac{(\theta_{T+1,d} - \theta_{*,d}^*)^2}{2\alpha_T K_{T,d}} + \sum_{t=2}^T (\theta_{t,d} - \theta_{*,d}^*)^2 \left[\frac{1}{2\alpha_t K_{t,d}} - \frac{1}{2\alpha_{t-1} K_{t-1,d}} \right]\end{aligned}\tag{77}$$

Given that $-\frac{(\theta_{T+1,d} - \theta_{*,d}^*)^2}{2\alpha_T (K_1)} \leq 0$ and $\frac{(\theta_{1,d} - \theta_{*,d}^*)^2}{2\alpha_1 (K_T)} \leq \frac{B_d^2}{2\alpha_1 (K_T)}$, we can bound it as:

$$\begin{aligned}& \sum_{t=1}^T \frac{(\theta_{t,d} - \theta_{*,d}^*)^2 - (\theta_{t+1,d} - \theta_{*,d}^*)^2}{2\alpha_t K_{t,d}} \\ & \leq \sum_{d=1}^D \frac{(\theta_{t,d} - \theta_{*,d}^*)^2}{2\alpha_t K_{t,d}}\end{aligned}\tag{78}$$

For the second term, we have:

$$\begin{aligned}& \sum_{t=1}^T -\frac{1 - K_{t,d}}{K_{t,d}} \widehat{m}_{t,d} (\theta_{t,d} - \theta_{*,d}^*) \\ & = \sum_{t=1}^T -\frac{1 - K_{t,d}}{K_{t,d}(1 - \beta_1^t)} \left(\sum_{i=1}^T (1 - \beta_{1,i}) \prod_{j=i+1}^T \beta_{1,j} \right) g_{t,d} (\theta_{t,d} - \theta_{*,d}^*) \\ & \leq \sum_{t=1}^T -\frac{1 - K_{t,d}}{K_{t,d}(1 - \beta_1^t)} \left(1 - \prod_{i=1}^T \beta_{1,i} \right) g_{t,d} (\theta_{t,d} - \theta_{*,d}^*) \\ & \leq \sum_{t=1}^T \frac{1 - K_{t,d}}{K_{t,d}(1 - \beta_1^t)} g_{t,d} (\theta_{t,d} - \theta_{*,d}^*)\end{aligned}\tag{79}$$

For the third term, we have:

$$\begin{aligned}
\sum_{t=1}^T \frac{\alpha_t}{2K_{t,d}} (\hat{g}_{t,d})^2 &\leq \sum_{t=1}^T \frac{\alpha_t}{2K_{t,d}} (\hat{m}_{t,d} + K_t(g_{t,d} - \hat{m}_{t,d}))^2 \\
&\leq \sum_{t=1}^T \frac{\alpha_t}{2K_{t,d}} ((1 - K_{t,d})\hat{m}_{t,d} + K_{t,d}g_{t,d})^2 \\
&\leq \sum_{t=1}^T \frac{\alpha_t}{2K_{t,d}} ((1 - K_{t,d})^2 \hat{m}_{t,d}^2 + K_{t,d}^2 g_{t,d}^2)
\end{aligned} \tag{80}$$

Collate all the items that we have:

$$R(T) \leq \sum_{d=1}^D \sum_{t=1}^T \frac{(\theta_{t,d} - \theta_{*,d}^*)^2}{2\alpha_t K_{t,d}} + \sum_{d=1}^D \sum_{t=1}^T \frac{1 - K_{t,d}}{K_{t,d}(1 - \beta_1^t)} g_{t,d}(\theta_{t,d} - \theta_{*,d}^*) + \sum_{d=1}^D \sum_{t=1}^T \frac{\alpha_t}{2K_{t,d}} ((1 - K_{t,d})^2 \hat{m}_{t,d}^2 + K_{t,d}^2 g_{t,d}^2) \tag{81}$$

Using Lemma 3 and Lemma 4. Therefore, from the assumption, $\|\theta_t - \theta^*\|_2^2 \leq B$, $\|\theta_m - \theta_n\|_\infty \leq B_\infty$, we have the following regret bound:

$$R(T) \leq \frac{B^2}{\alpha} \sum_{d=1}^D \sqrt{T} + \frac{2BG_\infty}{1 - \beta_1} \sum_{d=1}^D \|g_{1:T,d}\|_2^2 + \frac{\alpha G_\infty^2 (1 + (1 - \beta_1)^2)}{(1 - \beta_1)^2} \sum_{d=1}^D \|g_{1:T,d}\|_2^2 \tag{82}$$

B. Appendix 2

We performed extensive comparisons with other optimizers, including SGD [22], Adam[17], RAdam[20] and AdamW[21]. The experiments include: (a) image classification on Cifar dataset [18] with VGG [26], ResNet [13] and DenseNet [15], and image recognition with ResNet on ImageNet [6]; Hyperparameter tuning We performed a careful hyperparameter tuning in experiments. On image classification we use the following[35]:

- SGDF: We use the default parameters of Adam: $\beta_1 = 0.9$, $\beta_2 = 0.999$, $\epsilon = 10^{-8}$, and setting $\alpha = 0.3$.
- SGD : We set the momentum as 0.9 , which is the default for many networks such as ResNet and DenseNet. We search learning rate among $\{10.0, 1.0, 0.1, 0.01, 0.001\}$.
- Adam, RAdam: We search for optimal β_1 among $\{0.5, 0.6, 0.7, 0.8, 0.9\}$, search for α as in SGD, and set other parameters as their own default values in the literature.
- AdamW: We use the same parameter searching scheme as Adam. For other optimizers, we set the weight decay as 5×10^{-4} ; for AdamW, since the optimal weight decay is typically larger [21], we search weight decay among $\{10^{-4}, 5 \times 10^{-4}, 10^{-3}, 10^{-2}\}$.

1. Image classification with CNNs on Cifar

For all experiments, the model is trained for 200 epochs with a batch size of 128, and the learning rate is multiplied by 0.1 at epoch 150. We performed extensive hyperparameter search as described in the main paper. Here we report both training and test accuracy in Fig. SGDF not only achieves the highest test accuracy, but also a smaller gap between training and test accuracy compared with other optimizers.

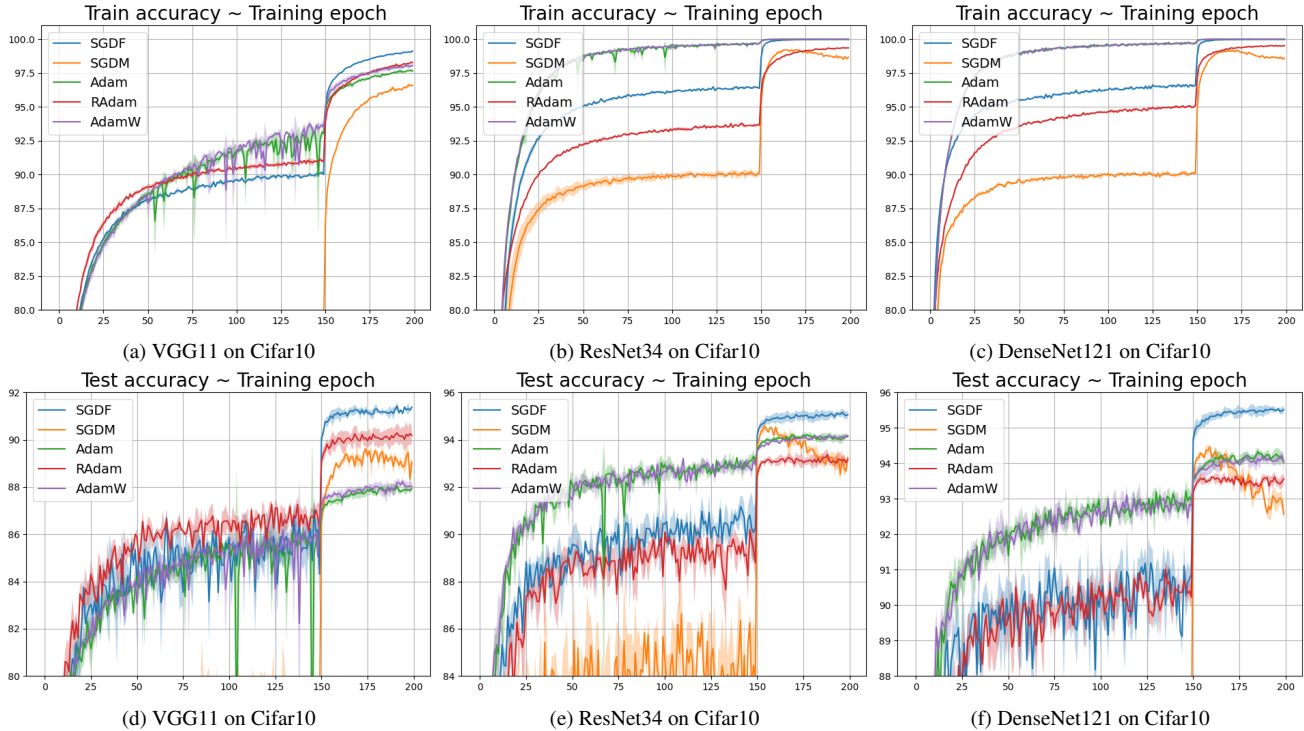


Figure 5. Training (top row) and test (bottom row) accuracy of CNNs on Cifar10 dataset. We report confidence interval ($\mu \pm \sigma$) of 3 independent runs.

2. Image Classification on ImageNet

We experimented with a ResNet18 on ImageNet classification task. For SGD, we use the same learning rate schedule as [13], with an initial learning rate of 0.1, and multiplied by 0.1 at epoch 30 and 60; for SGDF, we use an initial learning rate of

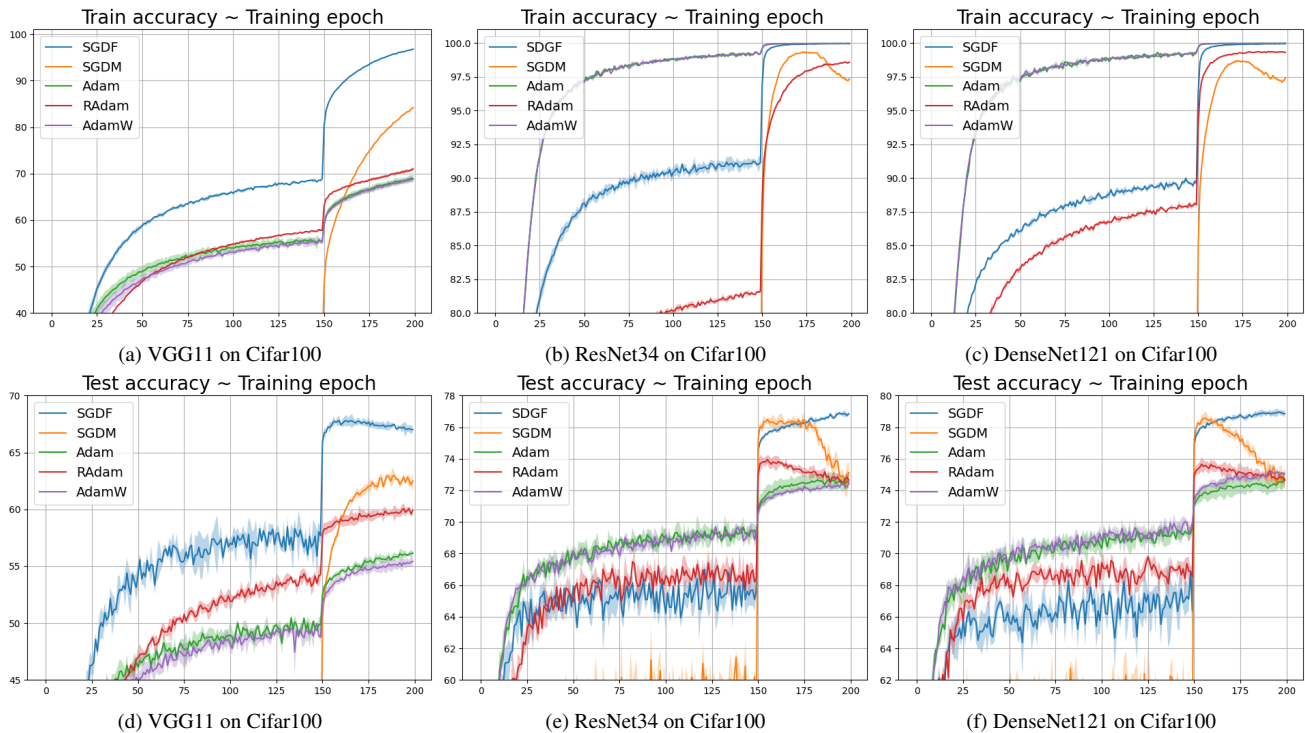


Figure 6. Training (top row) and test (bottom row) accuracy of CNNs on Cifar100 dataset. We report confidence interval ($[\mu \pm \sigma]$) of 3 independent runs.

0.3, and decayed it at epoch 30 and 60. Weight decay is set as 10^{-4} for both cases. To match the settings in [20]. As shown in Fig, SGDF achieves an accuracy very close to SGD, closing the generalization gap between adaptive methods and SGD. Meanwhile, when trained with a large learning rate (0.1 for SGD, 0.3 for SGDF), AdaBelief achieves faster convergence than SGD in the initial phase.

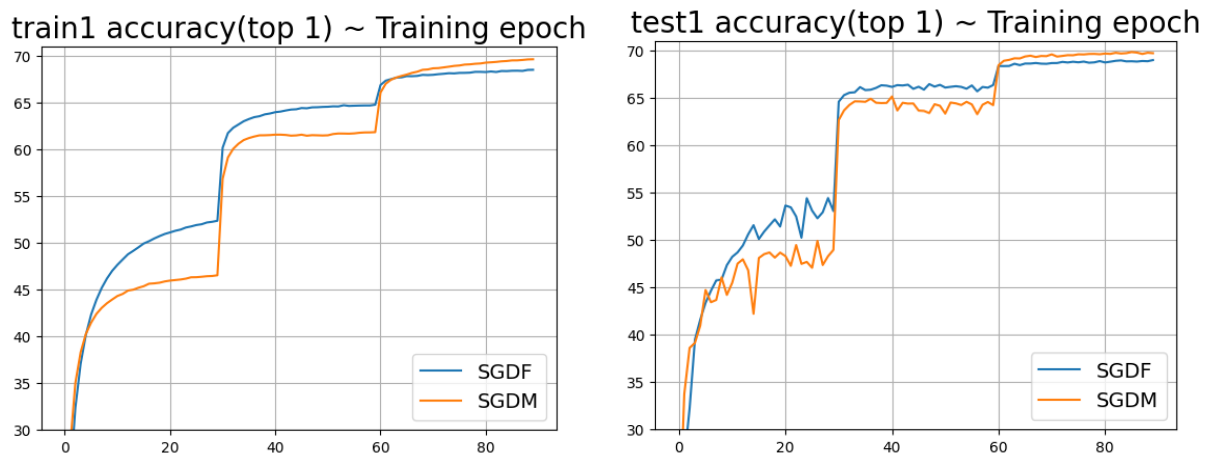


Figure 7. Training and test accuracy (top-1) of ResNet18 on ImageNet.